Bulg. J. Phys. **44** (2017) S71–S80

Probing for High Momentum Protons in ^{4}He via the ^{4}He$(e, e'p)^3$H Reaction

M.V. Ivanov[1], **J.M. Udías**[2], **S. Iqbal**[3], **N. See**[3], **K. Aniol**[3], **F. Benmokhtar**[4], **D. Finton**[4], **D. Higinbotham**[5], **SRC Collaboration**

[1]Institute for Nuclear Research and Nuclear Energy, Bulgarian Academy of Sciences, Sofia 1784, Bulgaria
[2]Grupo de Física Nuclear, Departamento de Física Atómica, Molecular y Nuclear, Universidad Complutense de Madrid, CEI Moncloa, Madrid, Spain
[3]California State University at Los Angeles, Los Angeles, California, USA
[4]Duquesne University, Pittsburgh, Pennsylvania, USA
[5]Thomas Jefferson National Accelerator Facility, Newport News, Virginia, USA

Received *31 July 2017*

Abstract. The relativistic distorted-wave impulse approximation (RDWIA) is used to describe the ^{4}He$(e, e'p)^3$H process. The ^{4}He ground state is determined within a relativistic mean field bound state fit to elastic electron scattering data. The nucleons are described by solutions of the Dirac equation with scalar and vector (S–V) potentials. The wave function of the outgoing proton is obtained by solving the Dirac equation with a S–V optical potential fitted to elastic proton scattering data on the residual nucleus. Experimental cross sections for the 3-body breakup ^{4}He$(e, e'p)^3$H up to $p_{\rm miss} = 0.632$ GeV/c at $x_B = 1.24$ and $Q^2 = 2$ (GeV/c)^2 are compared to the RDWIA calculations.

PACS codes: 24.10.-i, 25.10.+s, 25.30.Dh

1 Introduction

Quasielastic $(e, e'p)$ processes are a powerful tool to study bound nucleon properties. Indeed, coincidence $(e, e'p)$ measurements at quasielastic kinematics have provided over the years detailed information on the energies, momentum distributions and spectroscopic factors of bound nucleons. This is so because at quasielastic kinematics the $(e, e'p)$ reaction can be treated with confidence in the Impulse Approximation (IA), *i.e.*, assuming that the detected knockout proton absorbs the whole momentum (q) and energy (ω) of the exchanged photon (for reviews of the subject see [1] and references therein). The higher momentum transfer employed in the new experiments, made almost compulsory a fully relativistic treatment of the reaction mechanism. Within the most simple

relativistic framework, that parallells usual nonrelativistic approaches, a single-particle equation is used to compute both the bound and ejected nucleon wave function. The difference between the nonrelativistic approach employed in the 70's and 80's and the relativistic formalism lies thus, mainly, in the use of the Dirac equation instead of the Schrödinger one. The success of the simple Dirac single-particle picture in describing detailed features of the $(e, e'p)$ experimental data is intringuing and deserves close examination. In Ref. [2] are compared in details the nonrelativistic and relativistic impulse approximation to $(e, e'p)$.

Experimental access to proton momentum disributions is possible through the missing momentum observable, p_{miss}, in the $A(e, e'p)X$ reaction, $\mathbf{p}_X = \mathbf{p}_e - \mathbf{p}_{e'} - \mathbf{p}_p$, $p_{\text{miss}} = |\mathbf{p}_X|$. Interpretation of cross sections $\sigma(p_m)$ to deduce nucleon momentum distributions requires the inclusion of final state interactions (FSI) in the outgoing $(e'pX)$ system. Experiments E07006 [3] and E08009 [4] at the Jefferson National Accelerator Facility ran in February, March and April of 2011. Data for kinematic settings of 0.153 and 0.353 GeV/c missing momentum were obtained using electron beam currents between 47 μA to 60 μA, for E08009. The details for E08009 are described in Refs. [4–6]. In addition to these kinematic settings the Short Range Correlation (SRC) [3] experiment also obtained data at kinematic settings out to 0.632 GeV/c missing momentum including the two body break up channel p + triton. These higher missing momenta data were collected using about 4 to 5 μA electron beam currents but sufficient accumulated charge was measured to be able to extract cross sections beyond the original goal set for E08009. Moreover, the large acceptances of the Hall A spectrometers allowed for cross sections to be determined across a larger missing momentum range than the central value kinematic settings would suggest.

The electron spectrometer was fixed in angle and central momentum while the proton spectrometer's angles and central momenta were changed. The electron arm settings are in Table 1. The proton arm settings are in Table 2.

This paper contains the theoretical results obtained within RDWIA approximation and comparison with the experimental data from experiments E07006 and E08009.

Table 1. Electron spectrometer kinematic settings for E08009.

incident beam energy	4.4506 GeV
electron spectrometer angle	20.3°
electron spectrometer momentum	3.602 GeV/c
Q^2	2.0 (GeV/c)^2
Bjorken x_b	1.24

Table 2. Proton spectrometer settings.

Central $p_{\rm miss}$ [GeV/c]	θ_p [degrees]	Central momentum [GeV/c]
0.153	47.0	1.500
0.353	38.5	1.449
0.466	33.5	1.383
0.632	29.0	1.308

2 Formalism

In this section we summarize the formalism used to describe the coincidence $(e,e'p)$ reaction under the conditions defining the IA discussed in the Introduction. Figure 1 represents graphically the $(e,e'p)$ process. In this figure k_i^μ (k_f^μ) is the four-momentum of the incoming (outgoing) electron and q^μ is the four-momentum of the exchanged photon. The ejected proton four-momentum is denoted by P_F^μ. As represented in Figure 1 the electromagnetic transition is treated in Born approximation.

The differential cross-section for this process is then written as [7]:

$$\frac{d\sigma}{d\epsilon_f d\Omega_f dE_F d\Omega_F} = \frac{\delta(\epsilon_i + E_A - \epsilon_f - E_F - E_{A-1})}{(2\pi)^5} \times 4\alpha^2 \epsilon_f^2 E_F |\mathbf{P}_F| \, \overline{\sum} |W_{if}|^2 \,, \quad (1)$$

where $\overline{\Sigma}$ indicates sum (average) over final (initial) polarizations and

$$W_{if} = \int d\mathbf{x} \int d\mathbf{y} \int \frac{d\mathbf{q}}{(2\pi)^2} j_e^\mu(\mathbf{x}) e^{-i\mathbf{q}(\mathbf{x}-\mathbf{y})} \frac{(-1)}{q_\mu^2} J_N^\mu(\mathbf{y}) \,. \quad (2)$$

In this expression j_e^μ and J_N^μ stand for the electron and nuclear currents, respectively. The electron current is given by the well known point-like Dirac particle expression:

$$j_e^\mu(\mathbf{r}) = \bar{\psi}_f^e(\mathbf{r}) \gamma^\mu \psi_i^e(\mathbf{r}) \,, \quad (3)$$

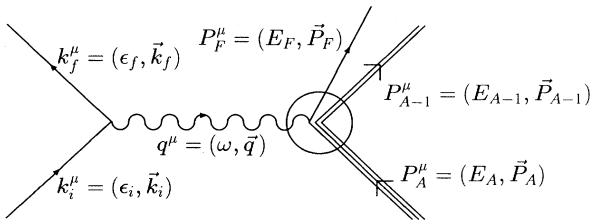

Figure 1. Schematic picture of the $(e,e'p)$ process.

where ψ_i^e, ψ_f^e stand for initial and final electron wave functions. For $(e, e'p)$ results on a light charge as this one (^{4}He) we do not introduce Coulomb distortion in the electron wave functions. Thus electron wave functions here are just simply plane waves. It corresponds with PWIA (Plane Wave Impulse Approximation) for the electrons, and DWIA (Distorted Wave Impulse Approximation), for the protons which see the nuclear potential.

In RDWIA [2, 7–20] and within an independent particle model picture, the nuclear current can be written in terms of the nucleon current operator $\hat{J}_N^\mu$

$$J_N^\mu(\mathbf{r}) = \bar{\psi}_F^N(\mathbf{r})\hat{J}_N^\mu\psi_B^N(\mathbf{r}) \ , \tag{4}$$

with ψ_B^N, ψ_F^N the wave functions for the initial bound nucleon and final nucleon, respectively, and $\hat{J}_N^\mu$ a nucleon current operator to be specified later. The bound state wave functions for the proton ψ_B^N are spinors with well defined angular momentum quantum numbers κ, μ corresponding to the shell under consideration. In coordinate space it is given by:

$$\psi_\kappa^\mu(\mathbf{r}) = \begin{pmatrix} g_\kappa(r)\phi_\kappa^\mu(\hat{r}) \\ \imath f_\kappa(r)\phi_{-\kappa}^\mu(\hat{r}) \end{pmatrix} \ , \tag{5}$$

which is eigenstate of total angular momentum with eigenvalue $j = |\kappa| - 1/2$,

$$\phi_\kappa^\mu(\hat{r}) = \sum_{m,\sigma}\langle lm\frac{1}{2}\sigma|j\mu\rangle Y_{lm}(\hat{r})\chi_\sigma^{\frac{1}{2}} \tag{6}$$

with $l = \kappa$ if $\kappa > 0$ and $l = -\kappa - 1$ if $\kappa < 0$. The functions f_κ, g_κ satisfy the usual coupled linear differential equations [7, 21, 22]. The mean field in the Dirac equation is determined through a Hartree procedure from a phenomenological relativistic lagrangian with scalar and vector S–V terms. The ^{4}He ground state is described with a relativistic mean field bound state fit to elastic electron scattering data.

The wave function of the detected proton ψ_F^N is a scattering solution of the time independent Dirac equation in configuration space

$$[\imath\boldsymbol{\alpha}\cdot\boldsymbol{\nabla} - \beta(M + U_{\rm S}) + E - U_{\rm V} - U_{\rm C}]\psi_F^N = 0 \ , \tag{7}$$

which includes S–V global optical potentials, obtained by fitting elastic proton scattering data [23].

This wave function is obtained as a partial wave expansion in configuration space

$$\psi_F^N(\mathbf{r}) = 4\pi\sqrt{\frac{E_F + M}{2E_F}}\sum_{\kappa,\mu,m} e^{-i\delta_\kappa^*}\imath^l\langle l\ m\ \frac{1}{2}\ \sigma_F|j\ \mu\rangle Y_{lm}^*(\hat{P}_F)\psi_\kappa^\mu(\mathbf{r}) \ , \tag{8}$$

where $\psi_\kappa^\mu(\mathbf{r})$ are four–spinors of the same form as that in Eq. (5), except that now the radial functions f_κ, g_κ are complex because of the complex potential.

It should also be mentioned that since the wave function Eq. (8) corresponds to an outgoing proton, we use the complex conjugates of the radial functions and phase shifts (the latter with the minus sign).

For the current operator we consider the two choices $cc1$ and $cc2$ introduced by de Forest [24] in momentum space

$$\hat{J}^{\mu}_{N}(cc1) = (F_1 + \bar{\kappa}F_2)\gamma^{\mu} - \frac{\bar{\kappa}F_2}{2M}(P_F + \bar{P}_I)^{\mu} \ , \tag{9}$$

$$\hat{J}^{\mu}_{N}(cc2) = F_1\gamma^{\mu} + i\frac{\bar{\kappa}F_2}{2M}\sigma^{\mu\nu}q_{\nu} \ , \tag{10}$$

where F_1 and F_2 are the nucleon form factors related in the usual way [25] to the electric and magnetic Sachs form factors of the dipole form. $\bar{P}_I$ in Eq. (9) is the four-momentum of the initial nucleon assuming on-shell kinematics [24]. The theoretical results presented in Section 3 are performed using $cc1$ current operator.

In nonrelativistic PWIA, the $(e,e'p)$ unpolarized cross section factorizes in the form

$$\left(\frac{d\sigma}{d\varepsilon_f d\Omega_f d\Omega_F}\right)^{\text{PWIA}} = E_F p_F f_{\text{rec}}\, \sigma_{ep}\, n_{\text{nr}}(\boldsymbol{p}_{\text{miss}}) \, , \tag{11}$$

where σ_{ep} is the bare electron-proton cross section usually taken as σ_{cc1} (or σ_{cc2}) of de Forest [24], and $n_{\text{nr}}(\boldsymbol{p}_{\text{miss}})$ is the *non relativistic momentum distribution* that represents the probability of finding a proton in the target nucleus with missing momentum $\boldsymbol{p}_{\text{miss}}$, compatible with the kinematics of the reaction. $\{\varepsilon_f, \Omega_f\}$ are the energy and solid angle corresponding to the scattered electron and $\Omega_F = (\theta_F, \phi_F)$ the solid angle for the outgoing proton. The factor f_{rec} is the usual recoil factor $f^{-1}_{\text{rec}} = |1 - (E_F/E_B)(\boldsymbol{p}_B \cdot \boldsymbol{p}_F)/p^2_F|$, being $\boldsymbol{p}_B$ and E_B the momentum and energy of the residual nucleus, respectively.

It is well known that the factorized result in Eq. (11) comes from an oversimplified description of the reaction mechanism. FSI, as well as Coulomb distortion of the electron wave functions, destroys in general factorization. In fact, most current descriptions of exclusive $(e,e'p)$ reactions involve unfactorized calculations. However, the simplicity of the factorized result makes it very useful to analyze and interpret electron scattering observables in terms of single particle properties of bound nucleons. Therefore it is common to quote *experimental reduced cross section* or *effective momentum distribution* on the basis of the experimental unpolarized cross section as

$$\rho^{\text{exp}}(\boldsymbol{p}_{\text{miss}}) = \frac{\left(\dfrac{d\sigma}{d\varepsilon_f d\Omega_f d\Omega_F}\right)^{\text{exp}}}{E_F p_F f_{\text{rec}}\, \sigma_{ep}} \, . \tag{12}$$

A similar expression can be used for the theoretical reduced cross section,

$$\rho^{\text{th}}(\boldsymbol{p}_{\text{miss}}) = \frac{\left(\dfrac{d\sigma}{d\varepsilon_f d\Omega_f d\Omega_F}\right)^{\text{th}}}{E_F p_F f_{\text{rec}}\, \sigma_{ep}}\,, \tag{13}$$

constructed from the the theoretical unpolarized $(e, e'p)$ cross section, independently of whether it is calculated within a relativistic or nonrelativistic formalism. We will say that the factorization property is satisfied by $\rho^{\text{th}}(\boldsymbol{p}_{miss})$ when the theoretical unpolarized cross section factors out exactly σ_{ep}, and then, the theoretical reduced cross section does not depend on it.

Due to the negative energy components of the bound proton wave function, factorization is not satisfied even in RPWIA [15]. However, if we neglect the contribution from the negative energy components, the unpolarized cross section factorizes to a similar expression as in Eq. (11). In a relativistic calculation, the assumptions written as

$$\psi_{\text{down}}(\boldsymbol{p}) = \frac{\boldsymbol{\sigma}\cdot\boldsymbol{p}_{\text{as}}}{E_{\text{as}}+M}\psi_{\text{up}}(\boldsymbol{p}) \tag{14}$$

with $E_{\text{as}} = \sqrt{\boldsymbol{p}_{\text{as}}^2 + M^2}$ and $\boldsymbol{p}_{\text{as}}$ the asymptotic momentum corresponding to each nucleon ("free" relationship with momenta determined by asymptotic kinematics at the nucleon vertex), set up the so-called effective momentum approximation with no scalar and vector terms (EMA-noSV) to which we will refer in what follows as EMA [13, 14]. In the relativistic case, factorization of the unpolarized cross section is broken even without FSI, due to the negative energy components of the bound nucleon wave function [15, 16]. A quantitative estimate of the breakdown of factorization is lacking for the relativistic case when taking into account FSI. It is important to stress that factorization may only be achieved assuming EMA and/or asymptotic projection, *i.e.*, neglecting dynamical enhancement of the lower components in the nucleon wave functions. This is *a priori* assumed within some nonrelativistic calculations.

3 Results

Experimental differential cross sections [3–6] are compared to relativistic distorted wave impulse approximation calculations of the Madrid theory group [2, 7–17]. The ^{4}He ground state is described with a relativistic mean field bound state fit to elastic electron scattering data. Nucleons are described by the Dirac equation with scalar and vector (S–V) potentials. The outgoing proton wave function is obtained by solving the Dirac equation with a S–V optical potential fitted to proton scattering on ^{3}H.

Vertex values of the incident electron's momentum at various positions within the target and the momenta of the scattered electron and ejected proton were

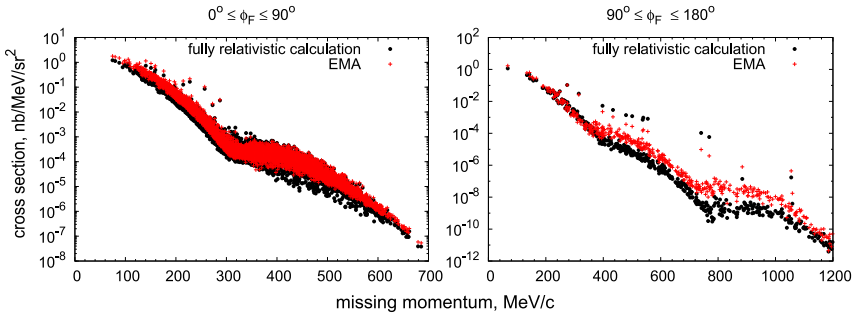

Figure 2. Central value of $p_{\rm miss} = 0.353$ GeV/c.

provided to the Madrid theory group for calculation of the cross section at each event vertex in the GEANT simulation. In Figure 2 are presented cross sections obtained within RWDIA (full relativistic calculations) and using the effective momentum approximation (EMA) [13, 14]. In Figure 2 are shown around 10% of all event vertices at central value of $p_{\rm miss} = 0.353$ GeV/c, where in the left panel are given results for values of the azimuthal angle of the outgoing proton $0^\circ \leq \phi_F \leq 90^\circ$ and in the right panel results at $90^\circ \leq \phi_F \leq 180^\circ$.

The GEANT simulation also contains the detected electron and proton momenta at the spectrometers' apertures. In this way the vertex cross section can be associated with the missing momentum at the apertures. The GEANT simulation includes external and internal bremsstrahlung. Preliminary results for the ratio of the experimental to the theoretical (integrated over the experimental acceptances for the full Madrid treatment) cross sections are shown in Figure 3. Experimental data, theoretical results, and more detailed discussion of the experimental setup and technics used in the analysis of the data of experiment E08009 will be presented in [6].

The data and calculations show the same missing momenta dependence on the measured or calculated cross section as a function of kinematic setting. Even though the same magnitude of $p_{\rm miss}$ is reached for different proton angles the cross section does not simply factor into a function of $p_{\rm miss}$. Good fits between the Madrid calculation and the data go out to about 420 MeV/c in missing momentum. Data and theory exhibit a break in the slope of the cross section between 300 and 400 MeV/c. The fact that are observed events in the triton region out to 632 MeV/c involves processes beyond the impulse approximation. Final state interactions of the outgoing proton may take a proton knocked out of a *proton–triton* cluster initially at a low value of p_p to appear as if its momentum at the vertex was $p_{\rm miss}$. This is accounted for to some extent by the optical potential treatment of the final *proton–triton* unbound state.

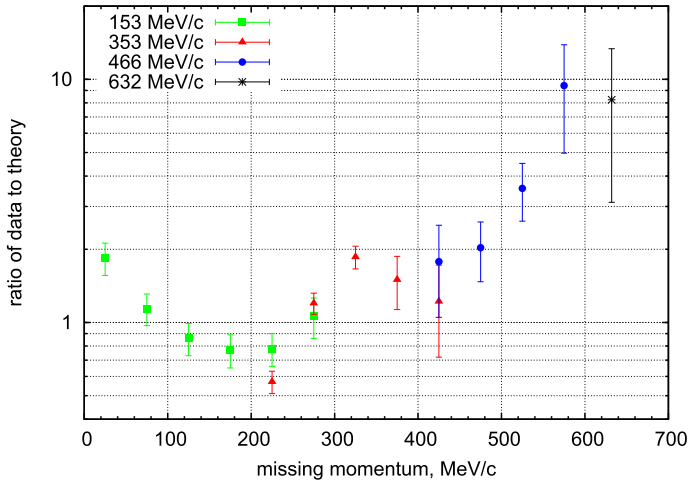

Figure 3. Preliminary results for the ratio of the experimental to the theoretical cross sections versus missing momentum. Squares are for the 153 MeV/c setting, triangles circles are for 353 MeV/c setting, circles are for the 466 MeV/c setting and stars are for the 632 MeV/c setting.

4 Conclusions

In this paper the RDWIA is used to describe the ^{4}He$(e,e'p)^3$H process. Nucleons in the ground state are described by solutions of the Dirac equation with S–V potentials. The wave function of the outgoing proton is obtained by solving the Dirac equation with a S–V optical potential fitted to elastic proton scattering data on the residual nucleus. Experimental cross sections for the 3-body breakup ^{4}He$(e,e'p)^3$H up to $p_{\rm miss} = 0.632$ GeV/c are compared to the RDWIA calculations.

The good agreement between the theory and data up to about $p_{\rm miss} = 420$ MeV/c is obtained. One expects high proton momentum to be attributable to the proton interacting with the remaining three nucleons which are not bound up as a triton ground state. In this case the tritons emitted at high $p_{\rm miss}$ may be a signature of secondary reactions allowing the three nucleon cluster to emerge as a bound state. Since the kinematics for the electron were chosen for $x_b = 1.24$, protons in more intimate interactions with neighbors than quasielastic conditions ($x_b \approx 1$) may favor secondary reactions leading to three nucleon clusters exiting as bound tritons.

Acknowledgments

This work was partially supported by the Bulgarian National Science Fund under Contracts No. DFNI-T02/19 and No. DFNI-E02/6.

References

[1] S. Boffi, C. Giusti, F.D. Pacati (1993) *Phys. Rep.* **226** 1; S. Boffi, C. Giusti, F. Pacati, M. Radici (1996) *"Electromagnetic Response of Atomic Nuclei"* (Oxford-Clarendon Press); J.J. Kelly (1996) *Adv. Nucl. Phys.* **23** 75.

[2] J.M. Udias, Javier R. Vignote, E. Moya de Guerra, A. Escuderos, and J.A. Caballero, "Recent Developments in relativistic models for exclusive $(e, e'p)$ reactions", Proceedings of the 5$^{\text{th}}$ Workshop on Electromagnetically Induced Two-Hadron Emission, ed. P. Grabmayr (Lund, 13–16 June 2001), arXiv:nucl-th/0109077.

[3] I. Korover *et al.* (2014) *Phys. Rev. Lett.* **113** 022501.

[4] Sophia Iqbal (2013) California State University, Los Angeles, unpublished, https://misportal.jlab.org/ul/publications/downloadFile.cfm?pub_id=13189.

[5] K.A.Aniol, N.Y See, and S. Iqbal (2013) unpublished, https://userweb.jlab.org/~aniol/e08009/iscan_corrections/SRCtgt.pdf.

[6] S. Iqbal *et al.* (2017) in preparation.

[7] J.M. Udías (1993) Ph.D. Thesis, Universidad Autónoma de Madrid.

[8] J.M. Udías, P. Sarriguren, E. Moya de Guerra, E. Garrido, J.A. Caballero (1993) *Phys. Rev. C* **48** 2731.

[9] J.M. Udías, P. Sarriguren, E. Moya de Guerra, E. Garrido, J.A. Caballero (1995) *Phys. Rev. C* **51** 3246.

[10] J.M. Udías, P. Sarriguren, E. Moya de Guerra, J.A. Caballero (1996) *Phys. Rev. C* **53** R1488.

[11] J.M. Udías, J.A. Caballero, E. Moya de Guerra, J.E. Amaro, T.W. Donnelly (1999) *Phys. Rev. Lett.* **83** 5451.

[12] J.M. Udías and Javier R. Vignote (2000) *Phys. Rev. C* **62** 034302.

[13] J.M. Udías, J.A. Caballero, E. Moya de Guerra, Javier R. Vignote, and A. Escuderos (2001) *Phys. Rev. C* **64** 024614.

[14] Javier R. Vignote, M.C. Martínez, J.A. Caballero, E. Moya de Guerra, and J.M. Udías (2004) *Phys. Rev. C* **70** 044608.

[15] J.A. Caballero, T.W. Donnelly, E. Moya de Guerra, and J.M. Udías (1998) *Nucl. Phys. A* **632** 323; (1998) *Nucl. Phys. A* **643** 189.

[16] M.C. Martínez, J.A. Caballero, and T.W. Donnelly (2002) *Nucl. Phys. A* **707** 83; (2002) *Nucl. Phys. A* **707** 121.

[17] R. Álvarez-Rodríguez, J. M. Udías, J.R. Vignote, E. Garrido, P. Sarriguren, E. Moya de Guerra, E. Pace, A. Kievsky, G. Salmè (2011) *Few-Body Syst* **50** 359—362.

[18] A. Picklesimer, J.W. Van Orden (1987) *Phys. Rev. C* **35** 266; (1989) **40** 290.

[19] Y. Jin, D.S. Onley (1994) *Phys. Rev. C* **50** 377.

[20] S.Gardner, J.Piekarewicz (1994) *Phys. Rev. C* **50** 2882.

[21] H. Überall, *Electron Scattering from Complex Nuclei*, Academic, N.Y., (1971). M.E. Rose, *Relativistic Electron Scattering*, Wiley, N.Y., (1961).

[22] B.D. Serot, J.D. Walecka (1986) *Adv. Nucl. Phys.* **16** 1.

[23] E. D. Cooper, S. Hama, and B. C. Clark (2009) *Phys. Rev. C* **80** 034605.

[24] Jr. T. de Forest (1983) *Nucl. Phys. A* **392** 232.

[25] J.D. Björken and S.D. Drell, *Relativistic Quantum Mechanics* (Mc Graw-Hill, N.Y. 1964).